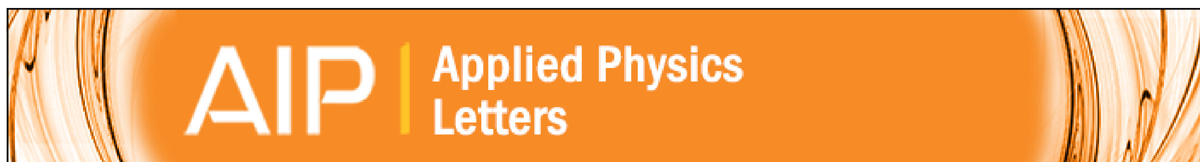

Transparent capacitors based on nanolaminate Al2O3/TiO2/Al2O3 with H2O and O3 as oxidizers

G. Z. Zhang, H. Wu, C. Chen, T. Wang, P. Y. Wang, L. Q. Mai, J. Yue, and C. Liu

Citation: Applied Physics Letters **104**, 163503 (2014); doi: 10.1063/1.4872470
View online: http://dx.doi.org/10.1063/1.4872470
View Table of Contents: http://scitation.aip.org/content/aip/journal/apl/104/16?ver=pdfcov
Published by the AIP Publishing

Articles you may be interested in

Interface-controlled high dielectric constant Al2O3/TiOx nanolaminates with low loss and low leakage current density for new generation nanodevices
J. Appl. Phys. **114**, 027001 (2013); 10.1063/1.4811810

Detailed leakage current analysis of metal–insulator–metal capacitors with ZrO2, ZrO2/SiO2/ZrO2, and ZrO2/Al2O3/ZrO2 as dielectric and TiN electrodes
J. Vac. Sci. Technol. B **31**, 01A109 (2013); 10.1116/1.4768791

Impact of ultrathin Al2O3 interlayer on thermal stability and leakage current properties of TiO2/Al2O3 stacking dielectrics
J. Vac. Sci. Technol. B **30**, 040601 (2012); 10.1116/1.4732737

Low leakage current in metal-insulator-metal capacitors of structural Al2O3/TiO2/Al2O3 dielectrics
Appl. Phys. Lett. **100**, 081101 (2012); 10.1063/1.3687702

Comparison of the self-cleaning effects and electrical characteristics of BeO and Al2O3 deposited as an interface passivation layer on GaAs MOS devices
J. Vac. Sci. Technol. A **29**, 061501 (2011); 10.1116/1.3628546

physicstoday
Comment on any *Physics Today* article.

This article is copyrighted as indicated in the article. Reuse of AIP content is subject to the terms at: http://scitation.aip.org/termsconditions. Downloaded to IP: 58.19.126.18 On: Thu, 24 Apr 2014 06:26:58

CrossMark click for updates

Transparent capacitors based on nanolaminate $Al_2O_3/TiO_2/Al_2O_3$ with H_2O and O_3 as oxidizers

G. Z. Zhang,[1] H. Wu,[1,a)] C. Chen,[1] T. Wang,[1] P. Y. Wang,[2] L. Q. Mai,[2] J. Yue,[1] and C. Liu[1,b)]
[1]*Key Laboratory of Artificial Micro- and Nano-structures of Ministry of Education, School of Physics and Technology, Wuhan University, Wuhan 430072, People's Republic of China*
[2]*State Key Laboratory of Advanced Technology for Materials Synthesis and Processing, WUT-Harvard Joint Nano Key Laboratory, Wuhan University of Technology, Wuhan 430072, People's Republic of China*

(Received 20 February 2014; accepted 11 April 2014; published online 23 April 2014)

Transparent capacitors with nanolaminate $Al_2O_3/TiO_2/Al_2O_3$ (ATA) hybrid dielectrics have been prepared on quartz glass by atomic layer deposition. The maximal capacitance density of 14 fF/μm^2 at 1 kHz was obtained. Moreover, an ultralow leakage current density of 2.1×10^{-9} A/cm^2 at 1 V was realized by using O_3 as the oxidizer. Fowler-Nordheim tunneling is the main mechanism of the leakage current at high fields, while several conduction mechanisms coexist at low fields. The AlZnO/ATA/AlZnO transparent capacitors exhibit an average optical transmittance of more than 80% in the visible range, which serve as good candidates for integration in transparent circuits. © *2014 AIP Publishing LLC*. [http://dx.doi.org/10.1063/1.4872470]

In recent years, great progresses have been made in development of transparent active matrix displays such as liquid crystal displays (LCDs) or organic light emitting devices (OLEDs).[1] In these circuits for displays, transparent thin film capacitors play an important role such as storage capacitors charging and discharging at the same frequency with thin film transistors (TFTs),[2,3] decoupling capacitors for microprocessors, filter and analog capacitors working with other electrical units to realize various logic functions.

Among various transparent electrodes, Al-doped ZnO (AZO) is promising because AZO films have many advantages such as low material cost, high chemical stability, high conductivity, and high optical transmittance.[4,5] Moreover, they are easily fabricated by various deposition methods. AZO films deposited by sputtering and pulsed laser deposition (PLD) methods have been used as electrodes in optoelectronic devices such as OLEDs,[6,7] photovoltaic cells,[8,9] TFTs,[10] and transparent storage capacitors.[11,12] However, the sputtering and PLD have some drawbacks such as high growth temperatures and physical damage to the film surface. As electrodes for capacitors, surface should be smooth enough to prevent electrons from accumulating in protuberant parts. Atomic layer deposition (ALD) is an alternative to grow high-quality AZO films.[13,14] It employs a surface controlled process to deposit thin films with atomic layer accuracy and offers many advantages such as *in situ* control of the film thickness and the impurity concentration. Moreover, the films deposited by ALD usually have smooth surface which are critical to make electrodes of capacitors.

In terms of dielectrics, many high-k materials have been investigated including Al_2O_3,[15] HfO_2,[16,17] ZrO_2,[18] TiO_2,[19,20] and various hybrid dielectric stacks.[21–23] But there are few reports about applications of these high-k dielectrics in transparent capacitors because of the relatively high resistivity of current transparent electrodes. In 2009, Xian and Yoon reported a kind of transparent capacitors with $Al_{0.016}In_{0.003}Zn_{0.981}O$ (AIZO) electrodes and a 200 nm thick $Bi_2Mg_{2/3}Nb_{4/3}O_7$ (BMN) pyrochlore film as dielectrics deposited by PLD, which showed a dielectric constant as high as 50–68.[11] However, the dielectric layer is too thick and the thickness cannot be accurately controlled by PLD, which limits its applications in integrated circuits. Among various dielectrics, TiO_2 is an ideal alternative material because of its transparency and a large dielectric constant of about 180 in crystallized rutile phase.[24] But the leakage current still remains a problem due to its relatively small bandgap (approximate 3.1 eV) and intrinsic n-type semiconductor properties. Many approaches have been adopted to suppress the leakage current. Among them, $Al_2O_3/TiO_2/Al_2O_3$ (ATA) laminate has been widely used because Al_2O_3 has a bandgap of about 8.9 eV and its excellent passivation properties usually lead to good interfacial qualities. In 2009, Woo *et al.* fabricated ATA capacitors with a low leakage current density of about 5×10^{-13} A/cm^2.[25] However, the electrodes of Ti/TiN limit its applications in transparent electronics.

In this work, the entire structures of capacitors (AZO/ATA/AZO) were *in situ* grown by ALD. The *in situ* method can form interfaces of very high quality, which is different from other methods that need post-annealing to improve electrical properties. In addition, *in situ* ALD grown method is promising to realize mass production and reduce the cost significantly. H_2O and O_3 were used as oxidizers, respectively, aiming to find which one can obtain better performance. The leakage mechanisms of the devices were also investigated.

As the bottom electrode, AZO films with a thickness of about 155 nm were deposited on the quartz glass at 200 °C by ALD (Beneq TFS-200). The AZO films were composed of 50 periods, and each period included 20 cycles of ZnO and 1 cycle of Al_2O_3. Diethyl zinc (DEZn) and deionized water were used as precursors to deposit ZnO films with a growth rate of 0.15 nm/cycle. Al_2O_3 films were grown using the precursors of trimethyl aluminum (TMA) and H_2O with a growth rate of 0.1 nm/cycle. Our previous work has reported the optimized growth conditions of ZnO and Al_2O_3.[26,27]

a)Electronic mail: H.Wu@whu.edu.cn
b)Electronic mail: Chang.Liu@whu.edu.cn

 © 2014 AIP Publishing LLC

This article is copyrighted as indicated in the article. Reuse of AIP content is subject to the terms at: http://scitation.aip.org/termsconditions. Downloaded to IP: 58.19.126.18 On: Thu, 24 Apr 2014 06:26:58

Afterward, a small part of AZO film was protected by kapton tape to serve as the probe position during subsequent electrical measurements. Then, $Al_2O_3/TiO_2/Al_2O_3$ thin films (with the thickness of 3/20/3 nm and 5/20/5 nm, respectively) were deposited. The Al_2O_3 dielectric films were prepared at 200 °C with 30 and 50 cycles for the thicknesses of 3 nm and 5 nm, respectively. The detailed growing conditions were the same as that of Al_2O_3 in growth of AZO films. Tetrakis-dimethylamido titanium (TDMAT) and oxidizers (O_3 or H_2O) were used to grown TiO_2 at 125 °C. For H_2O as the oxidizer, the growth rate is about 0.05 nm/cycle and the films were grown with 400 cycles. A typical ALD cycle consists of 2 s of the TDMAT pulse time, followed by 10 s of purge time, then 200 ms of H_2O pulse time, and 10 s of purge time. For O_3 as the oxidizer, the growth rate is about 0.04 nm/cycle and the total cycles are 500. In each cycle, the TDMAT pulse time is 2 s, followed by 10 s of purge time, then 1 s of O_3 pulse time, and 10 s of purge time. The average growth rates of films above were estimated by measuring the thicknesses of these films grown on silicon with specific cycles. The thicknesses were measured using a spectroscopic ellipsometer (J. A. Woollam alpha-SE). After that, another AZO films (with a thickness of 200 nm) were deposited as the top electrode. In comparison, AZO/Al_2O_3 (20 nm)/AZO and AZO/TiO_2 (20 nm)/AZO device structures were also fabricated. Standard photolithography and wet etching process were used to form capacitor areas. The final capacitors were approximately $100 \times 100\,\mu m^2$ in area. The capacitance density versus voltage (*C-V*) and leakage current density versus voltage (*I-V*) characteristics were measured by using a semiconductor device analyzer (Agilent B1500A). The optical transmittance was measured in a wavelength range of 300–800 nm by using a UV-VIS-NIR spectrophotometer (Varian Cary 5000).

Figure 1(a) shows the schematic diagram of transparent capacitors. To investigate the transparent characteristics, optical transmittance spectra of different device structures are shown in Fig. 1(b). An average optical transmittance over 80% in visible range was observed, which is valuable for storage capacitors in applications such as LCD, OLED, and solar cells. As seen from the inset of Fig. 1(b), the pattern of Wuhan University can be clearly observed through the transparent device.

Figure 2(a) shows the *C-V* characteristics of the AZO/Al_2O_3 (20 nm)/AZO structure when the voltage was varied from −2 V to 2 V. The capacitance density almost keeps constant at 3.4 fF/μm^2 from 1 to 100 kHz, which corresponds to a dielectric constant of 7.7. The inset of Fig. 2(a) shows the *C-V* curve of AZO/TiO_2 (20 nm)/AZO structure measured at 1 MHz. As shown, the capacitance density reached up to 32 fF/μm^2 at 0 V, corresponding to a dielectric constant of about 72. However, the leakage current is large (not shown). For Al_2O_3 dielectrics, the capacitance density drops significantly when the frequency varies from 100 kHz to 1 MHz. The dielectric loss at high frequencies could be attributed to the relatively high resistivity of AZO ($1.4 \times 10^{-3}\ \Omega$ cm). Figure 2(b) shows the *I-V* characteristics from −7 V to 7 V. The ultralow leakage current density is obtained, leading to very little dielectric loss at low frequencies (almost 3.4 fF/μm^2 from 1 kHz to 100 kHz). Therefore, Al_2O_3 films demonstrate excellent insulating properties and passivation abilities on AZO electrode. Along this line, a combination of Al_2O_3 and TiO_2 can exploit the advantages of both large dielectric constant of TiO_2 and excellent insulating properties of Al_2O_3.

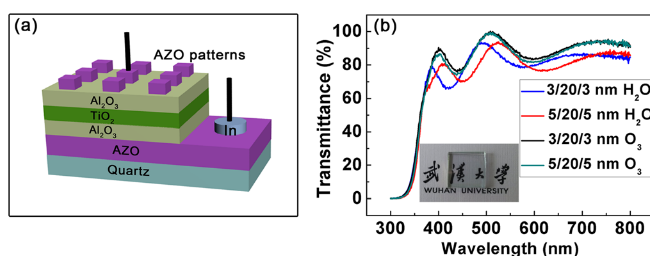

FIG. 1. (a) The schematic diagram of capacitors. (b) The optical transmittance spectra of devices with different $Al_2O_3/TiO_2/Al_2O_3$ structures. The inset of (b) is the photo image of capacitor device with the Chinese characters of "Wuhan University" on the background.

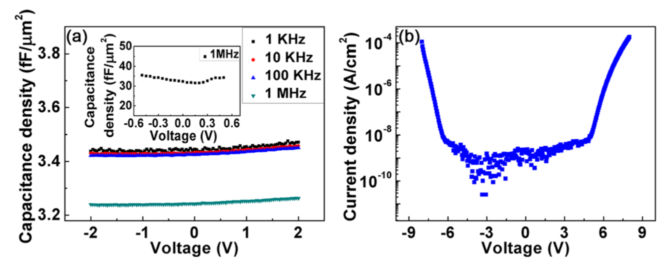

FIG. 2. Electrical characteristics of AZO/Al_2O_3 (20 nm)/AZO capacitors. (a) *C-V* results. (b) *I-V* results. The inset of (a) is the *C-V* results of AZO/TiO_2 (20 nm)/AZO measured at 1 MHz.

Figure 3 shows the *C-V* characteristics of the ATA (3/20/3 nm) and ATA (5/20/5 nm) samples with O_3 or H_2O as oxidizer, respectively. In the case of H_2O as the oxidizer, the capacitance density of ATA (3/20/3 nm) shows a maximal value of 14 fF/μm^2 ($\varepsilon_r = 41$) at 1 kHz and decreases to 11 fF/μm^2 ($\varepsilon_r = 32$) as the frequency increases to 1 MHz. However, the maximal capacitance density of ATA (5/20/5 nm) is reduced to 8.7 fF/μm^2 ($\varepsilon_r = 29$) at 1 kHz due to the increase of Al_2O_3 component. The frequency dispersion exists because of a relatively high leakage current density which are 9.6×10^{-5} A/cm^2 for ATA (3/20/3 nm) and 2.7×10^{-7} A/cm^2 for ATA (5/20/5 nm) at 1 V, as shown in Fig. 4. To decrease the leakage current, H_2O was replaced by O_3. This is better because O_3 is highly volatile and has stronger oxidizing ability than H_2O.[28,29] Particularly, in 2013, Ramos *et al.* found that the reaction between titanium isopropoxide and O_3 proceeds without intermediate surface hydroxyl species by *in situ* Fourier transform infrared spectroscopy and X-ray photoelectron spectroscopy.[30] Though the precursor is different, TiO_2 films with less amount of oxygen vacancies and hydroxyl residuals may be obtained by using O_3 as the oxidizer. As shown in Fig. 4, the leakage current densities at 1 V have been decreased to 1.1×10^{-6} A/cm^2 for ATA (3/20/3 nm) and 2.1×10^{-9} A/cm^2 for ATA (5/20/5 nm) due to the incorporation of O_3. For ATA structures using O_3 as the oxidizer, the ultralow leakage current yields a large reduction of frequency dispersion at low frequencies (1 kHz–100 kHz) as shown in Figs. 3(c) and 3(d). However, the capacitance densities are lower than that using H_2O as the oxidizer for the same ATA structures.

This article is copyrighted as indicated in the article. Reuse of AIP content is subject to the terms at: http://scitation.aip.org/termsconditions. Downloaded to IP: 58.19.126.18 On: Thu, 24 Apr 2014 06:26:58

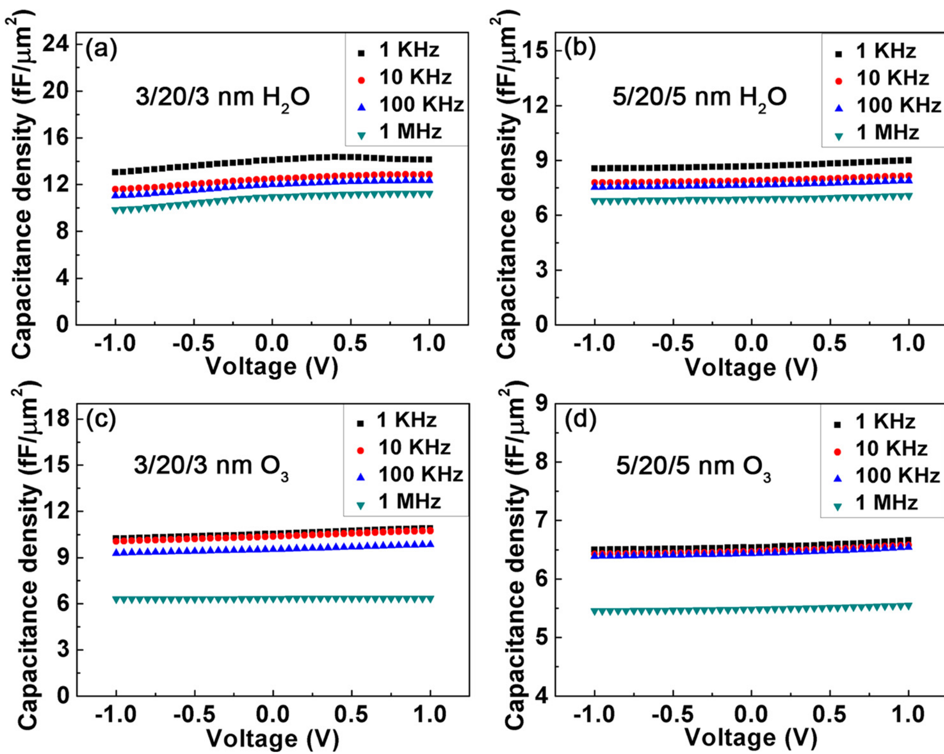

FIG. 3. *C-V* characteristics of ATA capacitors with different thicknesses and oxidizers.

The leakage current is proportional to the amount of defects in ATA dielectrics. The defects have twofold influences on the *C-V* properties. On the one hand, it can exacerbate the dielectric loss at low frequencies. On the other hand, these defects could provide inherent electric dipoles that can respond to extra electric field frequencies. Thus, the ATA structures with more defects (H_2O as oxidizer) exhibit higher capacitance density than that with fewer defects (O_3 as oxidizer).

It is important to understand the leakage mechanism because the leakage current through dielectric films is usually unavoidable. To investigate the conduction mechanism of the transparent capacitors, several models including Schottky emission, Frenkel-Poole (F-P) emission, and Fowler-Nordheim (F-N) tunneling[31] are used. Taken the AZO/Al_2O_3 (20 nm)/AZO structure into consideration, ohmic behavior is found to be dominant at a low field ($E < 2.55$ MV/cm), as shown in Fig. 5(a). However, the slope reaches 31 at high fields, which satisfies neither ohmic nor space-charge-limited-current (SCLC) mechanism. The inset of Fig. 5(a) shows the relationship between $\ln(J/E^2)$ and the reciprocal of the electric field (E^{-1}). When the field is above 2.5 MV/cm, a linear relationship is observed, which means that the conduction mechanism is governed by F-N tunneling at high fields. As for ATA dielectrics, 3/20/3 nm structures based on H_2O and O_3 are studied. Schottky and F-P emission models are widely applied to describe the leakage current of thin dielectric films at low or moderate electric fields.[32] If the conduction is governed by the Schottky emission at a constant temperature, the relationship of $\ln(J)$ vs $E^{1/2}$ should be linear. Similarly, $\ln(J/E)$ vs $E^{1/2}$ should have a linear relationship if the conduction is controlled by the F-P emission. Fig. 5(b) shows the Schottky plots of the leakage current with $\ln(J) \sim E^{1/2}$. The plots of both the ATA structures are linear at low fields. And the fitted relative

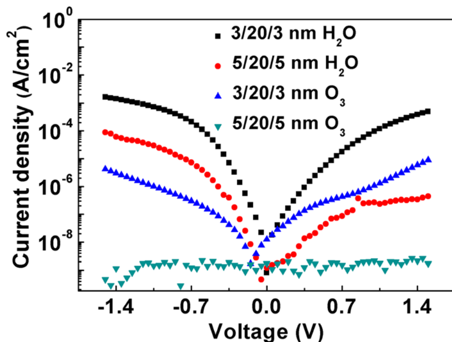

FIG. 4. *I-V* characteristics of ATA capacitors with different thicknesses and oxidizers.

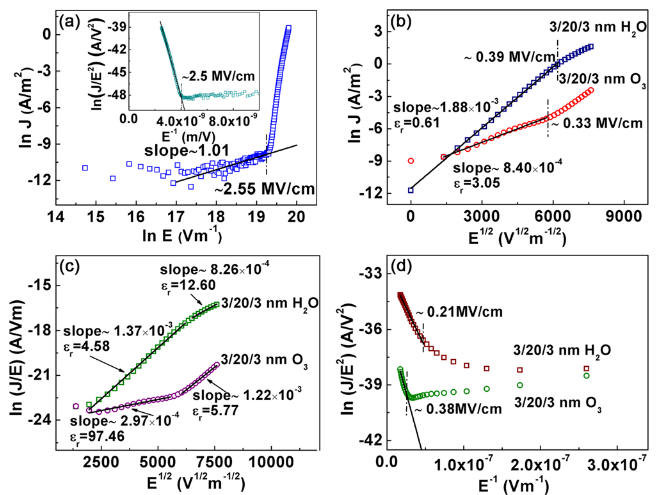

FIG. 5. (a) Ohmic plots of the leakage current of AZO/Al_2O_3 (20 nm)/AZO structure. The inset of (a) is F-N tunneling plots. (b), (c), (d) corresponding to Schottky, F-P emission, and F-N tunneling plots of ATA (3/20/3 nm) structures, respectively.

This article is copyrighted as indicated in the article. Reuse of AIP content is subject to the terms at: http://scitation.aip.org/termsconditions. Downloaded to IP: 58.19.126.18 On: Thu, 24 Apr 2014 06:26:58

dielectric constants are 0.61 and 3.05 for ATA based on H_2O and O_3, respectively. The values are not available compared with the experimental data (32 and 18, respectively). Fig. 5(c) shows the F-P plots with $\ln(J/E) \sim E^{1/2}$. The linear relationships are observed at different sections of the whole electric field range. But only the fitted dielectric constant of 12.6 may be available at very high frequencies (maybe several MHz). Therefore, neither Schottky nor F-P models govern the leakage current. There should be several mechanisms coexisting in the low fields. Figure 5(d) shows the relationship between $\ln(J/E^2)$ and E^{-1}. It is obvious that ATA (3/20/3 nm) structure using H_2O as the oxidizer follows the F-N tunneling when the field is above 0.21 MV/cm. F-N tunneling mechanism also happens when the field exceeds 0.38 MV/cm for ATA (3/20/3 nm) using O_3 as the oxidizer.

In ideal situation, there exists an Al_2O_3 barrier with 3 nm thickness between AZO and TiO_2 films. For pure Al_2O_3 (20 nm) as dielectrics, the barrier height is so big that there are almost no Schottky or F-P emissions happened in low field range just as Fig. 5(a) shows. But in ATA (3/20/3 nm) structures, Schottky and F-P emissions coexist in low field range, which can be attributed to the relatively high concentration of defects. It is probably related to oxygen vacancies in TiO_2 films and interfacial defects between Al_2O_3 and TiO_2 as well as interfacial states between electrode and dielectric layer. For ATA using H_2O as the oxidizer, there are more oxygen vacancies and hydrogen ions in TiO_2 films. And the overmuch oxygen vacancies can lead to more Ti^{4+} diffusion into Al_2O_3, which weakens the insulating of barriers and increases the probabilities of tunneling. Hence, the F-N tunneling happens at a relatively lower field ($E > 0.21$ MV/cm). While for ATA (3/20/3 nm) using O_3 as the oxidizer, reduction of oxygen vacancies and no hydroxides enhance the insulating properties of TiO_2. Hence, the F-N tunneling happens at relatively high fields ($E > 0.38$ MV/cm).

In conclusion, transparent capacitors have been fabricated on quartz glass by ALD method. *C-V* measurements show a maximal capacitance density of 14 fF/μm^2 corresponding to a dielectric constant of 41 at 1 kHz. By introducing O_3 as the oxidizer, a very low leakage current density of 2.1×10^{-9} A/cm^2 at 1 V was achieved. In addition, by analyzing different leakage mechanisms, we conclude that F-N tunneling is the main mechanism at high fields, while several conduction mechanisms coexist at low fields. The AZO/ATA/AZO transparent capacitors exhibit an average optical transmittance over 80% in the visible range, which may serve as possible candidates for integration in transparent circuits.

This work was supported by the NSFC under Grant Nos. 11074192, 11175135, 10904116, J1210061 and the foundation from CETC No. 46 Research Institute. Dr. Wu was supported by China Scholarship Council No. 201208420584. The authors would like to thank Z. Guo and X. Xu for the technical support.

[1]J. Meyer, S. Hamwi, M. Kroger, W. Kowalsky, T. Riedl, and A. Kahn, Adv. Mater. **24**, 5408 (2012).
[2]H. Frenzel, A. Lajn, and M. Grundmann, Phys. Status Solidi RRL **7**, 605 (2013).
[3]T.-J. Ha and A. Dodabalapur, Appl. Phys. Lett. **102**, 123506 (2013).
[4]H. Kim, M. Osofsky, S. M. Prokes, O. J. Glembocki, and A. Piqué, Appl. Phys. Lett. **102**, 171103 (2013).
[5]P. Banerjee, W.-J. Lee, K.-R. Bae, S. B. Lee, and G. W. Rubloff, J. Appl. Phys. **108**, 043504 (2010).
[6]S. H. Park, B. H. Lee, J. M. Shin, S.-Y. Jeong, S. Song, H. Suh, and K. Lee, Appl. Phys. Lett. **100**, 133306 (2012).
[7]J. Meyer, P. Görrn, S. Hamwi, H. H. Johannes, T. Riedl, and W. Kowalsky, Appl. Phys. Lett. **93**, 073308 (2008).
[8]H. Liu, Z. Wu, J. Hu, Q. Song, B. Wu, H. L. Tam, Q. Yang, W. H. Choi, and F. Zhu, Appl. Phys. Lett. **103**, 043309 (2013).
[9]N. Formica, D. S. Ghosh, A. Martinez-Otero, T. L. Chen, J. Martorell, and V. Pruneri, Appl. Phys. Lett. **103**, 183304 (2013).
[10]P. Ray and V. R. Rao, Appl. Phys. Lett. **102**, 064101 (2013).
[11]C.-J. Xian and S.-G. Yoon, J. Electrochem. Soc. **156**, G180 (2009).
[12]C.-M. Park, J.-H. Park, and S.-G. Yoon, J. Electrochem. Soc. **157**, G258 (2010).
[13]J. W. Elam, Z. A. Sechrist, and S. M. George, Thin Solid Films **414**, 43 (2002).
[14]J. W. Elam and S. M. George, Chem. Mater. **15**, 1020 (2003).
[15]P. Banerjee, I. Perez, L. Henn-Lecordier, S. B. Lee, and G. W. Rubloff, Nat. Nanotechnol. **4**, 292 (2009).
[16]S.-W. Kim, S. K. Lee, Y. D. Kim, and S. Kim, Appl. Phys. Lett. **96**, 262904 (2010).
[17]S. Jayanti and V. Misra, Appl. Phys. Lett. **99**, 222903 (2011).
[18]H. Spahr, C. Nowak, F. Hirschberg, J. Reinker, W. Kowalsky, D. Hente, and H.-H. Johannes, Appl. Phys. Lett. **103**, 042907 (2013).
[19]J. H. Han, S. Han, W. Lee, S. W. Lee, S. K. Kim, J. Gatineau, C. Dussarrat, and C. S. Hwang, Appl. Phys. Lett. **99**, 022901 (2011).
[20]Q. Xie, D. Deduytsche, M. Schaekers, M. Caymax, A. Delabie, X.-P. Qu, and C. Detavernier, Appl. Phys. Lett. **97**, 112905 (2010).
[21]D. A. Deen, J. G. Champlain, and S. J. Koester, Appl. Phys. Lett. **103**, 073504 (2013).
[22]G. Lee, B.-K. Lai, C. Phatak, R. S. Katiyar, and O. Auciello, Appl. Phys. Lett. **102**, 142901 (2013).
[23]C. Mahata, S. Mallik, T. Das, C. K. Maiti, G. K. Dalapati, C. C. Tan, C. K. Chia, H. Gao, M. K. Kumar, S. Y. Chiam, H. R. Tan, H. L. Seng, D. Z. Chi, and E. Miranda, Appl. Phys. Lett. **100**, 062905 (2012).
[24]K. Fröhlich, Mater. Sci. Semicond. Process. **16**, 1186 (2013).
[25]J.-C. Woo, Y.-S. Chun, Y.-H. Joo, and C.-I. Kim, Appl. Phys. Lett. **100**, 081101 (2012).
[26]T. Wang, H. Wu, C. Chen, and C. Liu, Appl. Phys. Lett. **100**, 011901 (2012).
[27]T. Wang, H. Wu, Z. Wang, C. Chen, and C. Liu, Appl. Phys. Lett. **101**, 161905 (2012).
[28]S. K. Kim, G.-J. Choi, S. Y. Lee, M. Seo, S. W. Lee, J. H. Han, H.-S. Ahn, S. Han, and C. S. Hwang, Adv. Mater. **20**, 1429 (2008).
[29]Y.-W. Kim and D.-H. Kim, Korean J. Chem. Eng. **29**, 969 (2012).
[30]K. B. Ramos, G. Clavel, C. Marichy, W. Cabrera, N. Pinna, and Y. J. Chabal, Chem. Mater. **25**, 1706 (2013).
[31]S. M. Sze, *Physics of Semiconductor Device*, 2nd ed. (Wiley, New York, 1981).
[32]H. Wu, J. Yuan, T. Peng, Y. Pan, T. Han, and C. Liu, Appl. Phys. Lett. **94**, 122904 (2009).

This article is copyrighted as indicated in the article. Reuse of AIP content is subject to the terms at: http://scitation.aip.org/termsconditions. Downloaded to IP: 58.19.126.18 On: Thu, 24 Apr 2014 06:26:58